J Mater Sci: Mater Med (2006) 17:697–707
DOI 10.1007/s10856-006-9680-1

Effect of carbonate content and buffer type on calcium phosphate formation in SBF solutions

S. Jalota · S. B. Bhaduri · A. C. Tas

Received: 4 September 2004 / Accepted: 24 October 2005

Coating of titanium-based biomedical devices with a layer of carbonated, apatitic calcium phosphate increases their bone-bonding ability. Simulated or synthetic body fluids (SBF) have the ability of forming apatitic calcium phosphates on the immersed titanium alloys within a few days to 2 weeks. Apatite-inducing ability of 5 M NaOH-etched surfaces of Ti6A14V strips (10 × 10 × 1 mm) were tested by using three different SBF solutions all concentrated by a factor of 1.5. SBF solutions used in this comparative study were: i) 4.2 mM HCO_3^- TRIS-HCl buffered SBF (*conventional* SBF or *c*-SBF), ii) 27 mM HCO_3^- TRIS-HCl buffered SBF (*Tas*-SBF), and iii) 27 mM HCO_3^- HEPES-NaOH buffered SBF (*revised* SBF or *r*-SBF). While the *c*-SBF of low carbonate ion concentration (4.2 mM) was quite sluggish in forming a coat layer on Ti6A14V strips after 1 week of soaking at 37°C, *Tas*-SBF with a HCO_3^- concentration exactly equal to that of human plasma (27 mM) was able to fully coat the immersed strips. *Tas*-SBF solution was able to coat even the vertically-suspended Ti6A14V strips in 1 week. The coated strips were characterized by using XRD, SEM, and FTIR. The differences in the coating morphology and surface coverage were assessed for each SBF solution of this study. *In vitro* **characteristics of as-**coated Ti6A14V strips was compared via the cell attachment, cell viability and total protein amount tests by using rat osteoblasts (7 F2). *In vitro* tests positively favored the calcium phosphate coatings of the TRIS-buffered, 27 mM HCO_3^- SBF over those of the *c*- and *r*-SBF solutions.

S. Jalota · S. B. Bhaduri · A. C. Tas (✉)
School of Materials Science and Engineering, Clemson University, Clemson, SC 29634, USA
e-mail: c_tas@hotmail.com

Introduction

SBF (simulated body fluid) solutions are able [1–3] to induce apatitic calcium phosphate formation on metals, ceramics or polymers (with proper surface treatments) immersed in them. SBF solutions, in close resemblance to the original Earle's (EBSS) [4] and Hanks' Balanced Salt Solution (HBSS) [5], were prepared to simulate the ion concentrations of human blood plasma. EBSS **formulation of 1943,** which has 26 mM of HCO_3^- and a Ca/P molar ratio of 1.8, **is relatively similar to today's** SBF [1–3] solutions. HBSS solution has a Ca/P ratio of 1.62. EBSS and HBSS solutions are derived from the physiological saline first developed by Ringer in 1882 [6]. It was recently reported that HBSS solutions are also able to slowly induce apatite formation on titanium [7], due to its low Ca/P ratio. For mimicking the ion concentrations of human blood plasma, SBF solutions have relatively low Ca^{2+} and HPO_4^{2-} concentrations of 2.5 mM and 1.0 mM, respectively [8]. pH values of SBF solutions were fixed at the physiologic value of 7.4 by using buffers, such as TRIS (tris-hydroxymethyl-aminomethane)-HCl [3] or HEPES (2-(4-(2-hydroxyethyl)-1-piperazinyl)ethane sulphonic acid)-NaOH [9, 10]. The buffering agent TRIS present in conventional SBF (*c*-SBF) formulations, for instance, was reported [11] to form soluble complexes with several cations, including Ca^{2+}, which further reduces the concentration of free Ca^{2+} ions available for the real time calcium phosphate coating. To the best of our knowledge, this behavior has not yet been reported for HEPES. HCO_3^- concentration in SBF solutions has been between 4.2 mM (equal to that of HBSS) [1] and 27 mM in revisited SBFs [12–14]. *c*-SBF, which was first popularized by Kokubo in 1990 [1], can be regarded as a TRIS/HCl-buffered variant of HBSS, whose Ca/P molar ratio was increased from 1.62 to 2.5. HBSS and *c*-SBF solutions have the same low carbonate ion concentrations

Table 1 Ion concentrations of human plasma and synthetic solutions, *mM*

	Blood plasma	Ringer[6]	EBSS[4]	HBSS[5]	*Kokubo-c*-SBF[1]	*Tas*-SBF[12]	*Bigi*-SBF[9]	*Kokubo-r*-SBF[10]
Na^+	142.0	130	143.5	142.1	142.0	142.0	141.5	142.0
K^+	5.0	4.0	5.37	5.33	5.0	5.0	5.0	5.0
Ca^{2+}	2.5	1.4	1.8	1.26	2.5	2.5	2.5	2.5
Mg^{2+}	1.5		0.8	0.9	1.5	1.5	1.5	1.5
Cl^-	103.0	109.0	123.5	146.8	147.8	125.0	124.5	103.0
HCO_3^-	27.0		26.2	4.2	4.2	27.0	27.0	27.0
HPO_4^{2-}	1.0		1.0	0.78	1.0	1.0	1.0	1.0
SO_4^{2-}	0.5		0.8	0.41	0.5	0.5	0.5	0.5
Ca/P	2.5		1.8	1.62	2.5	2.5	2.5	2.5
Buffer					TRIS	TRIS	HEPES	HEPES
pH	7.4	6.5	7.2–7.6	6.7–6.9	7.25–7.4	7.4	7.4	7.4

(i.e., 4.2 mM). Tas et al. [12, 13] **were** the first in 1999 to raise the carbonate ion concentration in a TRIS-HCl buffered SBF solution to 27 mM, while Bigi et al. [9] **were** the first to do the same in a HEPES-NaOH buffered SBF solution. Table 1 summarizes these SBF **compositions.** Eagle's minimum essential medium (MEM) [15] and Dulbecco's phosphate buffer saline (PBS) [16], which are commonly used in cell culture studies, may also be added to this table.

Dorozhkina et al. [17] underlined the influence of HCO_3^- concentration in an SBF solution on the morphology and thickness of calcium phosphate coatings formed. They compared two types of TRIS-free SBF solutions in that study; (i) one with 4.2 mM HCO_3^- and (ii) **another** SBF with 27 mM HCO_3^- **with** the solution pH **regulated** by bubbling CO_2. The most important result drawn from this study was: "increasing the HCO_3^- concentration in *c*-SBF from 4.2 to 27 mM resulted in the formation of homogeneous and much thicker carbonated hydroxyapatite layers" [17]. The same fact was also reported by Kim et al. [14] on PET substrates immersed into *r*-SBF. Dorozhkina et al. [17] emphasized that HEPES was rather unstable, in comparison to TRIS, and it easily lost some of the initially present dissolved carbonates. Kokubo et al. [10], who developed the HEPES-buffered *r*-SBF recipe, also reported that *r*-SBF would release CO_2 gas from the fluid, causing a decrease in HCO_3^- concentration, and an increase in pH value, when the storage period was long. Furthermore, they clearly stated that *r*-SBF would not be suitable for long-term use in the biomimetic coating processes owing to its instability [10]. To accelerate the SBF-coating processes, solutions equal to 1.5 times the ionic concentration of SBF were often used [18–20]. Habibovic et al. [21] prepared 5 × SBF-like solutions, without using any buffering agents and also removing K^+ and SO_4^{2-} ions from their solutions. Recently, Tas et al. [22] demonstrated the successful use of 10 × SBF-like (i.e., 25 mM Ca^{2+} and 10 mM HPO_4^{2-}) solutions in coating Ti6A14V surfaces at room temperature within 2 to 6 hours. Condensed (e.g., 5 or 10 times) solutions similar to SBF are prone to form precipitates with a higher carbonate content or with off-stoichiometric Ca/P molar ratios [23–25]. The **intention to coat** otherwise bioinert materials (such as, PET [14] or PTFE [26]) should have been the formation of bonelike, carbonated (not greater than 6 to 8% by weight) calcium phosphate layers with Ca/P molar ratios in the range of 1.55 to 1.67.

r-SBF was previously tested in coating collagen fibrils [27]. However, the *in vitro* apatite-inducing ability of neither *Tas*-SBF [12] nor *r*-SBF [10] has yet been reported on Ti6A14V substrates, in direct comparison to *c*-SBF. The motivation for the present study stems from our interest in finding experimental evidence to the following questions: (a) do the use of different buffers (TRIS or HEPES) in SBFs cause remarkable changes in the morphology or thickness of the calcium phosphate coat layers formed on Ti6A14V? (b) does the variation in HCO_3^- concentration affect the apatite-inducing ability of SBFs? and (c) how would the *in vitro* tests of rat osteoblast response diffrentiate between coatings formed by different SBFs?

Materials and methods

Ti6A14V strips (Grade 5, McMaster-Carr), with the dimensions of 10 × 10 × 1 mm, were used as substrates. The strips were first abraded with a #1000 SiC paper (FEPA P#1000, Struers), and then washed three times, respectively with acetone, ethanol, and deionized water in an ultrasonic bath. Each one of such strips was then immersed in 50 mL of a 5 M NaOH solution at 60°C for 24 hours in a glass bottle, followed by washing with deionized water and drying at 40°C.

Details of the SBF preparation routines are given in Table 2. Freshly prepared, 1.5× *c*-SBF [1], *Tas*-SBF [12], and *r*-SBF [10] solutions were used in coating experiments, unless otherwise noted. The order of addition of the reagents to water is given in the first column of Table 2. The reagent amounts were reported in columns 3 through 5 of Table 2.

Table 2 1.5 × SBF preparation

Order	Reagent	Weight (g per L)		
		c-SBF[1]	*Tas*-SBF[12]	*r*-SBF[1,10]
1	NaCl	12.0540	9.8184	8.1045
2	$NaHCO_3$	0.5280	3.4023	1.1100
3	Na_2CO_3	—	—	3.0690
4	KCl	0.3375	0.5591	0.3375
5	$K_2HPO_4 \cdot 3H_2O$	0.3450	—	0.3450
6	Na_2HPO_4	—	0.2129	—
7	$MgCl_2 \cdot 6H_2O$	0.4665	0.4574	0.4665
8	1 M HCl	15 mL	15 mL	—
9	HEPES	—	—	17.8920
10	$CaCl_2 \cdot 2H_2O$	0.5822	0.5513	0.5822
11	Na_2SO_4	0.1080	0.1065	0.1080
12	TRIS	9.0945	9.0855	—
13	1 M HCl	50 mL	50 mL	—
14	1 M NaOH	—	—	0.8 mL

NaOH-treated Ti6A14V strips were soaked at 37°C in 50 mL of 1.5× *c*-SBF, *Tas*-SBF and *r*-SBF in tightly sealed Pyrex® media bottles of 100 mL-capacity, for a period of 7, 14 and 21 days. All the SBF solutions were replenished at every 48 hours. Strips were removed from the SBF solutions at the end of respective soaking times, and washed with deionized water, followed by drying at 37°C. The strips were placed either "horizontally" on the base of the immersion bottles or dipped "vertically" into the solutions with a stainless steel wire [28]. Coated strips were examined by using an X-ray diffractometer (XRD; XDS 2000, Scintag Corp., Sunnyvale, CA), operated at 40 kV and 30 mA with monochromated Cu K α radiation. X-ray data were collected at 2θ values from 10° to 40° at a rate of 0.01° per minute. Fourier-transform infrared (FTIR) analyses were performed directly on the coated strips (Nicolet 550, Thermo-Nicolet, Wobum, MA). Surface morphology of the sputter-coated (w/Pt) strips was evaluated with a scanning electron microscope (SEM; S-4700, Hitachi Corp., Tokyo, Japan).

Calvarial rat osteoblast cells, designated 7 F2 (ATCC, Rockville, MD), were used for cell attachment studies on the SBF-coated strips. Cells were first grown at 37°C and 5% CO_2 in alpha MEM, augmented by 10% FBS. The culture medium was changed every other day until the cells reached a confluence of 90–95%. Osteoblasts were seeded at a density of 10^5 cells/cm^2. Cell cytotoxicity measurements were carried out after 24 hours, cell viability assessment was performed after 72 hours and total protein amount were measured after 7 days. Adhesion of the cells was quantified 24 hours after seeding. Trypan blue was added and the cells were counted using a light microscope **(BX60, Olympus, Tokyo, Japan).** Only cells that stain blue were deemed necrotic because of plasma membrane damage. For statistics, all experiments were performed in triplicate where $n = 3$. Analysis of variance was performed using the Tukey-Kramer multiple comparisons test. Osteoblast morphology after attachment was further examined using SEM. Prior to SEM investigations, samples were soaked in the primary fixative of 3.5% glutaraldehyde. Further, the cells were dehydrated with increasing concentrations of ethanol (50%, 75%, 90% and 100%) for 10 minutes each. Critical drying was performed according to the previously published procedures [29]. Samples were sputter-coated with Pt prior to the SEM imaging at 5 kV.

Results

Formation of a hydrated layer of sodium titanate on Ti6A14V strips was confirmed after 24 h of immersion in a 5 M NaOH solution at 60°C, as previously reported [30]. Alkali treatment also created a nano-scale roughness on the strip surfaces with, as shown in Figure 1(a). XRD analysis of the alkali-treated strips affirmed the presence of that hydrous sodium titanate layer, Figure 1(b). During our preliminary studies, we also prepared 1×SBF solutions (i.e., *c*-, *r*-, and *Tas*-SBF) and tested the formation of calcium phosphates (CaP) on alkali-treated Ti6A14V strips for 1 week of soaking at 37°C. There was almost no coating observed, regardless of the replenishment rate with these 1 × SBF solutions. For 1 ×SBF solutions, more than 3 weeks of soaking is required to observe only the onset of coating. To accelerate the coating process, 1.5 ×SBF solutions were prepared (Table 2).

When the Ti6A14V strips were placed horizontally (i.e., the strips were laying flat at the base of the bottles) in the 1.5 × SBF-immersion bottles, precipitates forming in the SBF solutions coalesced on the surfaces of the strips to form a grape bunch-like morphology. SEM micrographs of

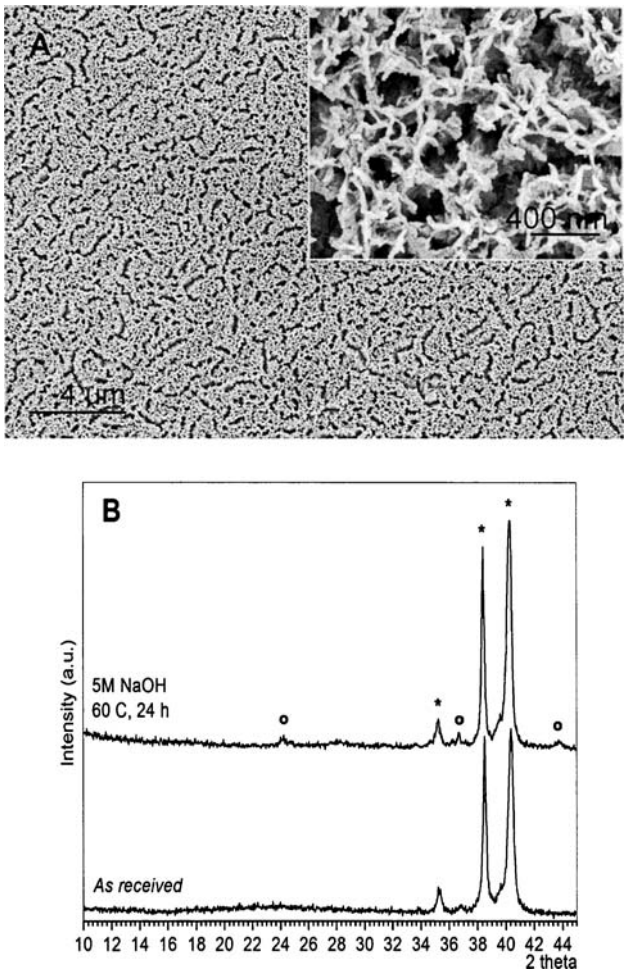

Fig. 1 5 M NaOH-treated Ti6A14V strips; (a) surface morphology, (b) XRD data, *Ti6A14V, ° Hydrous Na-titanate peaks.

Figures 2(a) through 2(c) show the surfaces of horizontally-placed strips soaked for 1 week, with replenishment on every other day. *c*-SBF solutions were not able to form a uniform coating (Fig. 2a), only occasional, agglomerated globules of CaP were observed on the strip surfaces. *Tas*-SBF solutions were found (Fig. 2b) to form an undercoat-like layer first, and then on top of it CaP globules were grown. *r*-SBF solutions were not able to form that undercoat layer (Fig. 2c). Figure 2(d), on the other hand, depicts the XRD data directly collected from the strip surfaces after 3 weeks of horizontal immersion in the respective SBF solutions. The sporadic and thin coating observed with the *c*-SBF solutions was not able to suppress the X-ray intensities of the peaks of Ti6A14V substrates. When the *c*-SBF solutions were not replenished during the immersion period (e.g., 1 week), there was almost no CaP coating. **Apatitic CaP coatings obtained by using the *Tas*-SBF solutions were able to reduce the intensities of the specific X-ray diffraction peaks of Ti6A14V substrates in comparison to those of *r*-SBF formulation, as shown in Fig. 2(d).** As its main disadvantage, horizontal placement did not allow the bottom faces of the strips to be coated.

The solution to the above problem was sought by vertically immersing the strips into the 1.5 × SBF solutions. Vertically-placed strips did not touch the bottom of the glass bottles, and they were placed at the halfway point along the entire height of the solution level. Vertical placement of the strips eliminated the problem of irregular formation of globules of apatitic CaP growing perpendicular to the coating surface, in all three SBF solutions tested [28]. Vertically-placed strips were also coated on both sides. SEM micrographs given in Figures 3(a) through 3(c) show the drastic improvement in the coating uniformity (in comparison to horizontal placement, Figs. 2(a)–2(c)), after 1 week in the SBFs. *c*-SBF solutions with 4.2 mM HCO_3^- again yielded a thin layer of calcium phosphate (CaP) coating, Fig. 3(a), in comparison to *Tas*-SBF solutions, Fig. 3(b). As seen in Fig. 3(a), CaP globules were formed in *c*-SBF solutions at the end of 1 week, but they were not able to completely cover the available surface. The micro-morphology difference between the CaP coatings of *Tas*- and *r*-SBF solutions was quite significant, Figs. 3(b) and 3(c).

XRD traces of the vertically-placed, 1 week-coated Ti6A14V strips are given in Figure 3(d). *c*-SBF solutions still formed a lesser quantity of apatitic CaP on the strips as compared to those formed by the *Tas*- and *r*-SBF. There was again no coating observed on Ti6A14V strips **in solutions without replenishment.** These data clearly showed that (a) the carbonate ion concentration in 1.5 × SBF solutions of pH 7.4 must be raised to the level of human blood plasma, i.e., 27 mM, to form a coating layer which fully covers the available strip surface in about 1 week, (b) the geometrical placement of the samples in SBF solutions has a strong effect on the morphology of the coatings, and (c) nano-morphology of the coatings obtained in *r*-SBF solutions were significantly different than those obtained in *c*- and *Tas*-SBF solutions.

The initial progress of the SBF-coating, as a function of soaking time, on vertically-placed Ti6A14V strips was also studied. SEM micrographs of Figures 4(a) to 4(d) demonstrated the morphology differences between the CaP coatings of *Tas*- and *r*-SBF solutions, both having 27 mM HCO_3^-, after 2 and 4 days of soaking. In TRIS-HCl buffered SBF solutions (*c*- and *Tas*- SBF), the increase in HCO_3^- concentration from 4.2 to 27 mM significantly enhanced the coating kinetics. HEPES-NaOH buffered SBF solutions (i.e., *r*-SBF), on the other hand, were far from reproducing that characteristic interlocking, needle- or plate-like nano-morphology of the coatings of TRIS-buffered SBFs. FTIR data of the 3 weeks-soaked samples showed that all the coatings were **consisting** of carbonated (CO_3^{2-} ion absorption bands seen at 1470-1420 and 875 cm^{-1}) calcium phosphates, Figure 4(e). The absence of the stretching and the vibrational modes of the O-H group at 3571 and 639 cm^{-1} confirmed

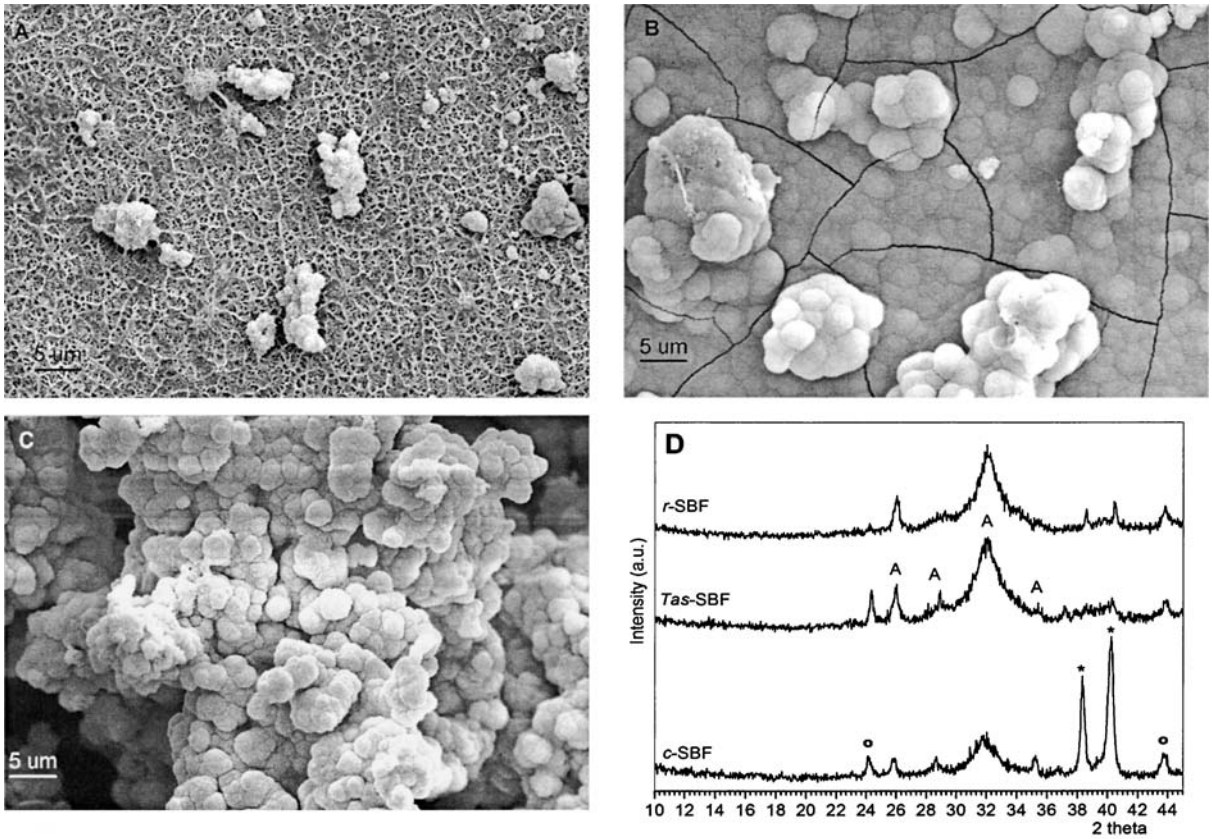

Fig. 2 Horizontally-soaked Ti6A14V strips, 1 week; (a) *c*-SBF, (b) *Tas*-SBF, (c) *r*-SBF, (d) XRD traces: A: apatitic CaP, *Ti6A14V, °hydrous Na-titanate peaks.

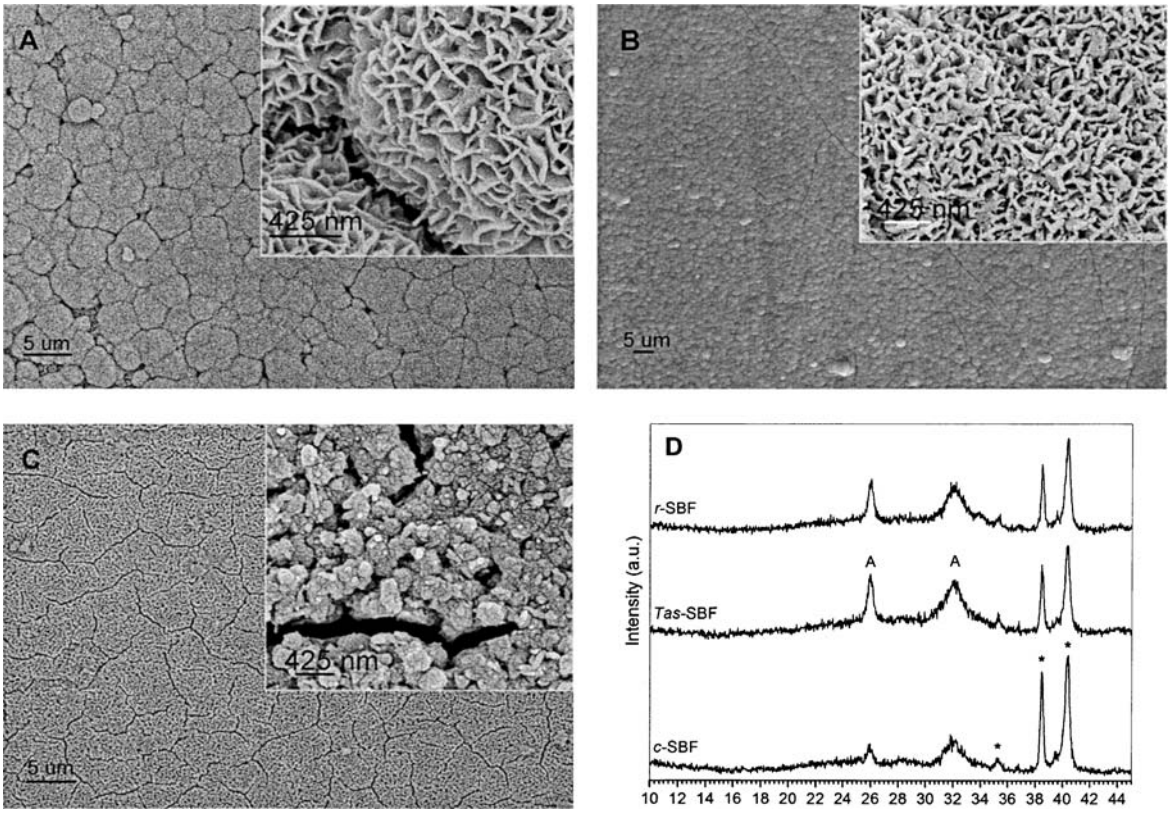

Fig. 3 Vertically-soaked Ti6A14V strips, 1 week; (a) *c*-SBF, (b) *Tas*-SBF, (c) *r*-SBF, (d) XRD data; A: apatitic CaP, *Ti6A14V, °hydrous Na-titanate peaks.

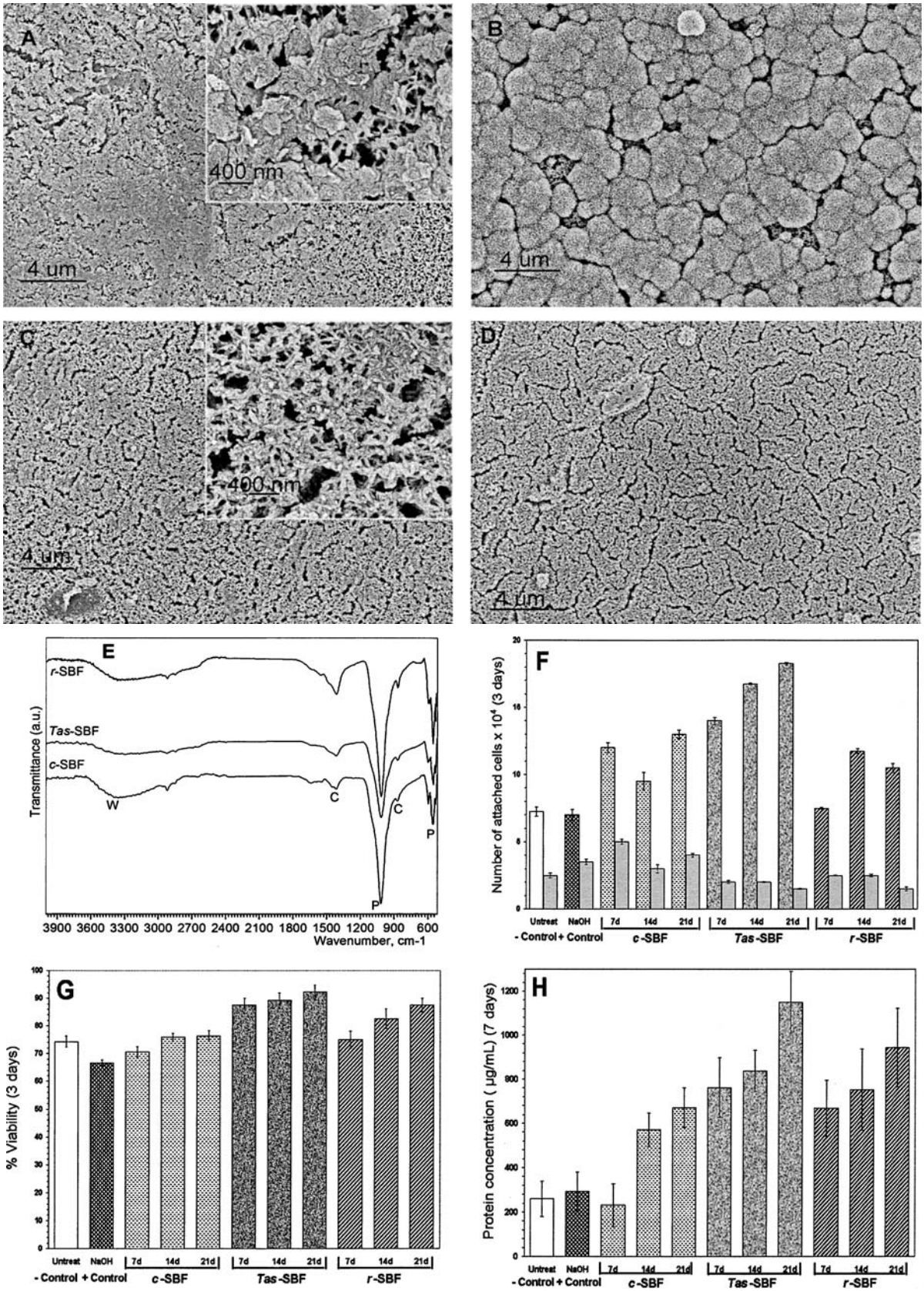

Fig. 4 (a) 2 days in *Tas*-SBF, (b) 4 days in *Tas*-SBF, (c) 2 days in *r*-SBF, (d) 4 days in *r*-SBF (e) FTIR data of CaP coatings; W: water, C: carbonate, P: phosphate bands, (f) number of osteoblasts attached on the CaP coatings of different SBFs after 3 days, solid grey bars = dead cells, (g) cell viability for *c*-, *Tas*- and *r*-SBF coatings after 3 days, (h) protein concentration results for different SBFs after 7 days.

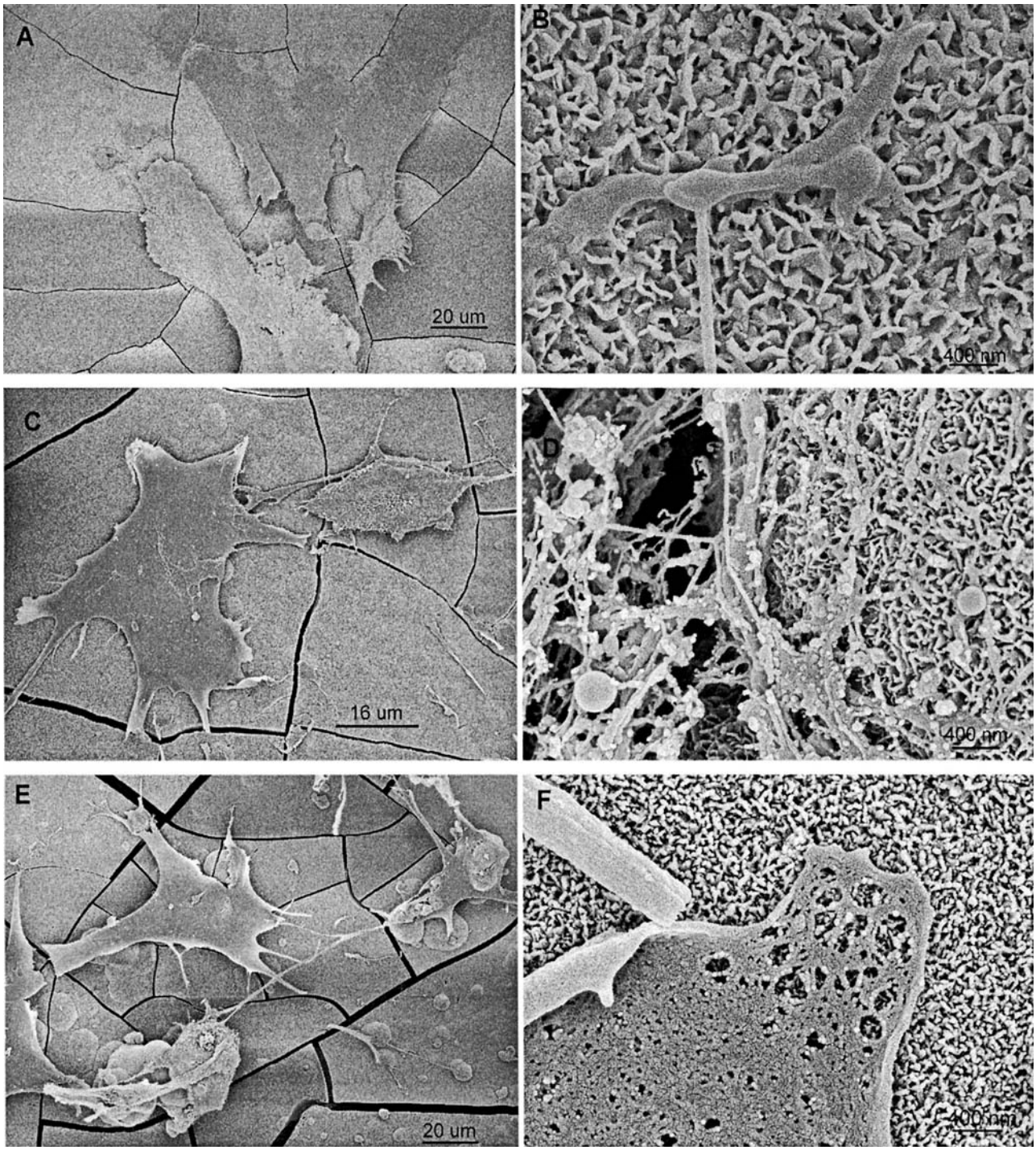

Fig. 5 SEM micrographs for the osteoblast attachment/adhesion on the CaP coatings (3 weeks of soaking time) of different SBF solutions, (a)−(b): *c*-SBF, (c)−(d): *Tas*-SBF, (e)−(f): *r*-SBF.

that these coating might not simply be named as "hydroxyapatite." From the FTIR data alone, it is rather difficult to distinguish between the coatings of different SBF solutions.

Rat osteoblasts showed significant differences in terms of the number of attached cells, cell viability, and protein concentration, as presented in Figures 4(f) through 4(h), between the apatitic calcium phosphate layers obtained by using the SBF solutions of this study. The number of attached cells, %viability, and protein concentration were all found to yield the highest values in the case of using a 27 mM HCO_3^--containing, TRIS-HCl buffered SBF solution (i.e., *Tas*-SBF). Osteoblast attachment on the surfaces of the SBF-coatings (on 3 weeks-soaked samples) was monitored by SEM, and given in Figures 5(a) through 5(f). Osteoblasts

were attached to the surfaces of the CaP coatings of all the SBF solutions tested here, however, the high-magnification pictures showed significant differences in osteoblast proliferation. The apatitic surfaces created by *Tas*-SBF solutions were found to be the most viable for osteoblasts to attach and grow in comparison to those of induced by *c*- and *r*-SBF.

Discussion

If CO_2 gas is bubbled through an aqueous solution of 2.5 mM $CaCl_2{\cdot}H_2O$, it would start precipitating sub-micron particles of $CaCO_3$ within few hours [31]. CO_2 bubbles cause the formation of carbonic acid, H_2CO_3, which subsequently dissociate into HCO_3^- and CO_3^{2-}. The reversal of these dissociation reactions will cause the release of CO_2 gas out of the solution, and a slight increase in solution pH. Marques et al. [25] have explained the buffering effect of HCO_3^-/CO_3^{2-} pair. However, an addition of 27 mM $NaHCO_3$ to the above solution can eliminate the necessity of bubbling CO_2, and it would again form $CaCO_3$ precipitates [32]. Then, if one adds 1 mM Na_2HPO_4 into this solution, it will precipitate calcium phosphates instead of $CaCO_3$. This solution has a Ca/P molar ratio of 2.50, with an ionic strength of 75 mM. It is saturated with respect to the formation of apatitic calcium phosphates, and it contains Ca^{2+}, HPO_4^{2-}, HCO_3^-, Na^+, and Cl^- ions. When the pH of the above solution is brought down to the range of 5 to 6, for instance, by adding tiny droplets of dilute HCl, it will only precipitate $CaHPO_4{\cdot}2\ H_2O$ [33]. If the pH value of that solution is kept at the physiological value of 7.4 or higher, it would precipitate carbonated, apatitic calcium phosphates. Over the pH range of 6.2 to 10, HCO_3^- is the most stable carbonate species in aqueous solutions. The precipitation of carbonated, apatitic calcium phosphates from such a solution may be described by the following reaction [34]:

$$(10-x-y)Ca^{2+} + (6-x-y)HPO_4^{2-} + yHCO_3^- + 2H^+ + 2OH^- = Ca_{10-x-y}[(HPO_4)_x(CO_3)_y(PO_4)_{6-x-y}](OH)_{2-x} + (8-x)H^+. \quad (1)$$

According to the above scheme, HPO_4^{2-} and CO_3^{2-} ions compete for the PO_4^{3-} tetrahedra. The charge imbalance created by these substitutions will be compensated by the Ca-vacancies. Monovalent Na^+ **and K^+ ions, as well as the divalent Mg^{2+} ions,** will also substitute over a certain fraction of the Ca-sites. **In SBF-based CaP coating on Ti6A14V substrates (or on ceramics and polymers), Na^+, K^+ and Mg^{2+} ions will also participate in the complex chemistry of the formed apatitic CaP [13].** Bone mineral, having extremely small sizes of biological apatite crystals (i.e., 20 to 30 nm), contains substantial amounts of CO_3^{2-} (4 to 8 wt%), 0.5% Mg^{2+}, 0.7% Na^+, and is about 10% Ca-deficient with the accompanying increase in reactivity related to this condition [35]. Precipitation of apatitic calcium phosphates may also be accompanied by a slight pH decrease (Eq^n 1). All the precipitated apatitic calcium phosphate powders, therefore, possess, some kind of Ca-deficiency, HPO_4^{2-} and CO_3^{2-} ions in their crystal structures. The addition of 5 mM K^+ and/or 0.5 mM SO_4^{2-} ions into a solution as described above do not change the nature of the precipitates formed. Increasing the amount of Na^+ and Cl^- ions to the levels present in human blood plasma (i.e., 142 and 103 mM, respectively) would just increase the ionic strength of the new solution. *c*- and *Tas*-SBF have the same ionic strength values, i.e., 160.5 mM, whereas *r*-SBF has a significantly lower value of 149.5 mM. Theoretically, if a solution has a low ionic strength, this means that the ionic diffusion will be enhanced in such a solution. In a solution of low ionic strength and high ionic diffusion, more nucleation sites are present for the precipitation reactions. CO_2 is released from an aqueous solution at a faster rate if the solution has a low ionic strength [25]. The presence of NaCl in human blood plasma is for the purpose of fixing the ionic strength at the value of 149.5 mM. On the other hand, if one increases the ionic strength of an SBF solution to above, e.g., 1100 mM, its rate of CO_2 release would be slowed down significantly [22]. If one adds 1.5 mM Mg^{2+} into the above solution, it is known that this may slow down the growth rate of apatitic calcium phosphates, favoring instead the formation of poorly-crystallized calcium phosphates [21].

Adjusting the pH of concentrated calcium phosphate solutions to 7.4 can readily be achieved by using organic buffers. For this purpose, the use of TRIS, $(HOCH_2)_3CNH_2$, has been a good choice [1, 12]. TRIS is a base and its buffering action comes from the following reaction:

$$(HOCH_2)_3CNH_2(aq) + H_2O(1) = (HOCH_2)_3CNH_3^+ (aq) + OH^-(aq). \quad (2)$$

This is also known as the TRIS/TRISH$^+$ buffer system, and the slow addition of HCl to this system gives the user the ability to **maintain** the pH value of solutions over the range of 7.2 to 7.4. Formulations of *c*- and *Tas*-SBF solutions used TRIS-HCl as the buffering agent. TRIS/TRISH$^+$ system has a well-known proton buffering capacity [36]. This trait of TRIS becomes especially important for incorporating aqueous HCO_3^- ions into the structures of apatitic calcium phosphates in the form of CO_3^{2-} ions, as described in equation (1). Moreover, a working pH of 7.4 is near the lower end of the buffering capacity of TRIS [36], and this facilitates the formation of CaP clusters in SBF solutions. HEPES, $C_8H_{18}N_2O_4S$,

on the other hand, is known to have a lower buffering capacity at pH 7.4 in comparison to TRIS [37, 38].

An amorphous calcium phosphate (ACP) precursor is always present during the precipitation of apatitic calcium phosphates from highly supersaturated solutions [39]. Posner et al. [35] proposed that the process of ACP formation in solution first involved the formation of $Ca_9(PO_4)_6$ clusters, which then aggregated randomly to produce the larger spherical particles or globules (as seen in Figs. 2 to 4), while the intercluster space being filled with water. Such clusters (with a diameter of about 9.5 Angstrom [39] are the transient solution precursors to the formation of calcium-deficient, carbonated apatitic calcium phosphate precipitates as described in equation (1). Onuma et al. [40] have demonstrated, by using dynamic light scattering, the presence of such calcium phosphate clusters from 0.7 to 1.0 nm in size even in transparent SBF**-like TRIS-buffered solutions of pH 7.4**. They reported that CaP clusters were present in SBF even when there was no precipitation. Since these nanoclusters are always present in SBF solutions, the insertion of a suitable alkali-treated Ti6A14V surface into the solutions triggers the hexagonal packing [40] of those nanoclusters to form apatitic CaP precipitates. ACP should also be present together with the apatitic CaP, as confirmed by the previous TEM studies performed on SBF-coating layers [3, 40]. The role of alkali-treated Ti6A14V surfaces in stimulating the SBF-coating process has been explained by Kokubo et al. [3]. Continuation of this phase separation process from the SBF solutions will be conditional upon the smooth supply of Ca^{2+}, HPO_4^{2-} and HCO_3^- ions to the metal-solution interface. These colloidal precipitates (as a result of the hexagonal packing of nanoclusters [40]) are formed by a homogeneous nucleation process. The presence of these initial precipitates within the solution further accelerates the coarsening of the newly deposited calcium phosphate globules.

TRIS or HEPES-buffered SBF solutions (1.5 × SBF) of 27 mM HCO_3^- concentration were able to form those surface-attached precipitates by the end of 2nd or 3rd day of soaking at 37°C. However, when the HCO_3^- concentration was lower (i.e., 4.2 mM; *c*-SBF) in the SBF, the rate of formation of these precipitates is decreased. Since the Ca/P molar ratio of the SBF solutions were 2.50, they are not stable against carbonated, apatitic CaP or OCP (octacalcium phosphate; $Ca_8(HPO_4)_2(PO_4)_4{\cdot}5H_2O$) precipitation when the solution pH is higher than 6.3 [12, 23]. With the advance of precipitate formation the level of supersaturation decreases, CaP precipitate formation comes to a halt, and hence this is where one needs replenishing the SBFs. A certain fraction of HCO_3^- is lost as $CO_2(g)$, followed by an increase in solution pH to above 7.5, which decreases the level of supersaturation of the solution [25]. This explains the lesser amount of coating formed on Ti6A14V strips when the solutions were not replenished, let's say, for 1 week. These pH increases in *r*-SBF were slightly higher than those observed in *Tas*-SBF. HEPES-buffered SBF solutions were not able to retain HCO_3^- ions to the extent that the TRIS-buffered SBF solutions did [17].

c- and *Tas*-SBF solutions did not exhibit a significant difference in the micro-morphology **and topography** of the apatitic CaP coatings they produced. TRIS-SBFs always produced round globules consisting of 'needle-like, intermingling, interlocking nanosize calcium phosphates' on the Ti6A14V strips (Figs. 3(a) and 3(b)). The reason for not seeing this commonly observed microstructure in the coatings of *r*-SBF (Fig. 3(c) and Fig. 4(d)) is difficult to enunciate. Bigi et al. [9] previously used a HEPES-buffered 27.0 mM HCO_3^- SBF solution to coat gelatin films. The SEM micrographs reported by Bigi et al. [9] showed nearly spherical aggregates, which resembled closely to the morphology of Ti6A14V strips coated in the present study with *r*-SBF. The buffer used in an SBF solution might have a significant influence on the morphology of its resultant coatings. The following questions still need to be answered by further research in this field. Could the use of S-rich HEPES (i.e., $C_8H_{18}N_2O_4S$) cause this alone? Could the use of Na_2CO_3, instead of $NaHCO_3$, in the *r*-SBF preparation recipes affect the precipitate morphology? If there is an inevitable morphology difference between the coatings of *Tas*- and *r*-SBF solutions, then could this be also reflected in their chemical compositions? Could the coatings of *r*-SBF solutions be OCP instead of apatitic calcium phosphate [42]?

Cracks observed in the SBF coatings **may be related to** the **hydrated** nature of those CaP deposits. Since Posner's clusters already have H_2O molecules in their intercluster spaces [40, 43], the aggregates of such clusters forming the nanoporous coat layers on Ti6A14V surfaces will also entrap a sizable amount of water. As long as the coating is thin **and does not cover the entire metal surface,** those drying cracks **are not expected to** be observed (Figs. 3(a) and 4(b)). With an increase in coating thickness, water entrapped would not readily escape during low-temperature drying, and deep cracks **are** observed (Figs. 3(b) and 4(d)) **[21]. The hydrous Na-titanate layers [31], placed onto Ti6A14V surfaces by soaking them in NaOH solutions, may also have a role in the formation of CaP coating cracks upon final drying. Moreover,** the significant thermal expansion mismatch between the Ti6A14V substrates and the CaP coat layers **could** also contribute to this defect.

Osteoblast behavior is sensitive to biochemical and topographical features (i.e., microarchitecture) of their substrate. The ideal and most preferred surface used by osteoblasts *in vivo* is the osteoclast resorption pit [44]. However, one may speculate that the surfaces of nanoporous, apatitic CaP coatings formed in an SBF solution at 37°C and pH 7.4 represents **biocompatible and non-toxic** substrates for the osteoblasts to respond to. The cytotoxicity, % viability and the protein content histograms given in Figures 4(f) to 4(h)

clearly showed that the CaP-coated (in *Tas*-SBF) Ti6A14V strips always performed better than either bare Ti6A14V or NaOH-treated TiA14V strips, **as well as those coated with *c*-SBF and *r*-SBF solutions.** Rat osteoblasts were able to easily differentiate between CaP coatings coming from different SBF solutions. **The main difference between the TRIS-buffered *c*- and *Tas*-SBF solutions was in their carbonate content.** In other words, osteoblasts favored a "TRIS-buffered SBF solution of 27 mM HCO_3^-" over the other SBFs of this study. **The improved osteoblast response to the CaP coatings of *Tas*-SBF can therefore be considered to arise mainly from the differences in SBF solution chemistry, and as seen in the SEM micrographs of Figs. 5(a) to 5(f) the topographical features of both the coatings are essentially the same.** It was quite interesting to note in Figure 4(h) that the adsorbed protein concentration measured in 7-days soaked samples of *Tas*-SBF was even higher than those of 21-days soaked in *c*-SBF solution. It is a well-known fact that the surface chemistry of a material determines the initial *in vitro* interactions of proteins, such as fibronectin with integrin cell-binding domains, which in turn regulate the cell adhesion process. Osteoblast response to the CaP surfaces of this study can be regarded as the sum of their ability to attach, proliferate, and differentiate. In the attachment stage, osteoblast filopodia explore the substrate topography for areas to which a greater surface area of the cell can adhere. These filopodia are used in sensing the substrate, and they extend over significant distances to find areas appropriate for attachment [45]. SEM micrographs of Figures 5(a), 5(c) and 5(e) revealed the extension of filopodia. Cracking of coatings became more pronounced in this case due to the critical point-drying of the seeded cells.

On coating surfaces, cells were flattened and spread with clear actin fibers associated with vinculin adhesion plaques (Fig. 5). The SEM micrograph of Fig. 5(d), recorded on a *Tas*-SBF-coated Ti6A14V surface, clearly showed the actin cytoskeleton and the stress fibers. On the other hand, the micrographs of 5(b) and 5(f) displayed the vinculin adhesion plaque formation on samples produced by using *c*-SBF and *r*-SBF, respectively. Cells are seen to produce fewer adhesion plaques while still in the process of migration than once permanently settled in place [46]. Sun et al. [47] exposed cells to calcium phosphate particles and reported that HA particles (100 nm) or β-TCP particles (100 nm) inhibited the growth of primary rat osteoblasts, while causing an increase in their expression of alkaline phosphatase [48]. In addition, Pioletti et al. [49] observed a decrease in growth, viability, and synthesis of extracellular matrix in primary rat osteoblasts that were exposed to β-TCP particles (1–10 μm) or $CaHPO_4{\cdot}2H_2O$ particles (1–10 μm). A 90% decrease in viability was reported by Pioletti et al. [49] when evaluated using a Live-Dead assay similar to what we have used in the present study. The absence of such effects **in this work** proved the biocompatible nature of **all** the SBF-coatings studied.

Conclusions

This study, for the first time, enabled the direct comparison of HEPES- and TRIS-buffered solutions (*r*- and *Tas*-SBF) of 27 mM HCO_3^- with one another, as well as with the TRIS-buffered, 4.2 mM HCO_3^- SBF solution (*c*-SBF), in terms of their apatite-inducing ability on Ti6A14V strips. The findings are: 1) A difference in coating morphology between the HEPES- and TRIS-buffered SBF solutions, both of 27 mM HCO_3^-, was found. HEPES-buffered SBF solutions (*r*-SBF) formed more solution precipitates in comparison to TRIS-buffered SBF solutions (*Tas*-SBF); that would limit their long term use in coating substrates. 2) The nominal carbonate ion concentration of an SBF solution influenced its CaP deposition rate; the apatitic CaP forming rate of *c*-SBF on NaOH-treated Ti6A14V was inferior to that of *Tas*-SBF. 3) SBF-coating process was considerably affected by the placement geometry of the metallic substrates in the SBF solutions; horizontally-placed Ti6A14V strips exhibited a growth pattern of CaP deposits extending upwards in the solution, while the vertically-soaked strips were coated more uniformly without such artifacts of sedimentation. 4) *In vitro* rat osteoblast culture tests performed on the apatitic CaP coatings were found to favor the TRIS-buffered, 27 mM SBF solutions (i.e., *Tas*-SBF) by yielding increased cell viability and protein concentrations.

Acknowledgments This work, a part of the MSc thesis of Sahil Jalota, was partially supported by an NSF grant **no. 0409119.** Authors are also cordially grateful for the generous help of Prof. Thomas Boland of the Department of Bioengineering in performing the *in vitro* experiments.

References

1. T. KOKUBO, *J. Non-Cryst. Solids* **120** (1990) 138.
2. T. KOKUBO, *Acta Mater.* **46** (1998) 2519.
3. T. KOKUBO, H.-M. KIM, M. KAWASHITA and T. NAKAMURA, *J. Mater. Sci. Mater. M.* **15** (2004) 99.
4. W. EARLE, *J. N. C. I.* **4** (1943) 165.
5. J. H. HANKS and R. E. WALLACE, *Proc. Soc. Exp. Biol. Med.* **71** (1949) 196.
6. S. RINGER, *J. Physiol.* **4** (1880–1882) 29.
7. L. FRAUCHIGER, M. TABORELLI, B. O. ARONSSON and P. DESCOUTS, *Appl. Surf. Sci.* **143** (1999) 67.
8. H.-M. KIM, H. TAKADAMA, F. MIYAJI, T. KOKUBO, S. NISHIGUCHI and T. NAKAMURA, *J. Mater. Sci. Mater. M.* **11** (2000) 555.
9. A. BIGI, E. BOANINI, S. PANZAVOLTA and N. ROVERI, *Biomacromolecules* **1** (2000) 752.
10. A. OYANE, K. ONUMA, A. ITO, H.-M. KIM, T. KOKUBO and T. NAKAMURA, *J. Biomed. Mater. Res.* **64 A** (2003) 339.

11. A. P. SERRO and B. SARAMAGO, *Biomaterials* **24** (2003) 4749.
12. D. BAYRAKTAR and A. C. TAS, *J. Eur. Ceram. Soc.* **19** (1999) 2573.
13. A. C. TAS, *Biomaterials* **21** (2000) 1429.
14. H.-M. KIM, K. KISHIMOTO, F. MIYAJI, T. KOKUBO, T. YAO, Y. SUETSUGU, J. TANAKA and T. NAKAMURA, *J. Mater. Sci. Mater. M.* **11** (2000) 421.
15. H. EAGLE, *Science* **122** (1955) 501.
16. R. DULBECCO and M. VOGT, *J. Exp. Med.* **106** (1957) 167.
17. E. I. DOROZHKINA and S. V. DOROZHKIN, *Coll. Surface. A*, **210** (2002) 41.
18. Y. E. GREISH and P. W. BROWN, *J. Biomed. Mater. Res.* **52** (2000) 687.
19. H. TAKADAMA, H.-M. KIM, T. KOKUBO and T. NAKAMURA, *ibid.* **57** (2001) 441.
20. S. H. RHEE and J. TANAKA, *Biomaterials* **20** (1999) 2155.
21. P. HABIBOVIC, F. BARRERE, C. A. VAN BLITTERSWIJK, K. DE GROOT and P. LAYROLLE, *J. Am. Ceram. Soc.* **85** (2002) 517.
22. A. C. TAS and S. B. BHADURI, *J. Mater. Res.* **19** (2004) 2742.
23. E. I. DOROZHKINA and S. V. DOROZHKIN, *J. Biomed. Mater. Res.* **67A** (2003) 578.
24. S. V. DOROZHKIN, E. I. DOROZHKINA and M. EPPLE, *Cryst. Growth Des.* **4** (2004) 389.
25. P. A. A. P. MARQUES, M. C. F. MAGALHAES and R. N. CORREIA, *Biomaterials* **24** (2003) 1541.
26. L. GRONDAHL, F. CARDONA, K. CHIEM, E. WENTRUP-BYRNE and T. BOSTROM, *J. Mater. Sci. Mater. M.* **14** (2003) 503.
27. E. K. GIRIJA, Y. YOKOGAWA and F. NAGATA, *Chem. Lett.* **7** (2002) 702.
28. B. FENG, J. Y. CHEN, S. Q. QI, L. HE, J. Z. ZHAO and X. D. ZHANG, *Biomaterials* **23** (2002) 173.
29. T. J. WEBSTER, R. W. SIEGEL and R. BIZIOS, *Biomaterials* **20** (1999) 1221.
30. P. LI, I. KANGASNIEMI, K. DE GROOT and T. KOKUBO, *J. Am. Ceram. Soc.* **77** (1994) 1307.
31. D. RAUTARAY, K. SINHA, S. S. SHANKAR, S. D. ADYANTHAYA and M. SASTRY, *Chem. Mater.* **16** (2004) 1356.
32. O. GRASSMANN and P. LOEBMANN, *Biomaterials* **25** (2004) 277.
33. R. TANG, C. A. ORME and G. H. NANCOLLAS, *J. Phys. Chem. B* **107** (2003) 10653.
34. T. LEVENTOURI, B. C. CHAKOUMAKOS, N. PAPANEARCHOU and V. PERDIKATSIS, *J. Mater. Res.* **16** (2001) 2600.
35. A. S. POSNER and F. BETTS, *Acc. Chem. Res.* **8** (1975) 273.
36. J. PRATT, J. D. COOLEY, C. W. PURDY and D. C. STRAUS, *Curr. Microbiol.* **40** (2000) 306.
37. B. R. VAN DYKE, D. A. CLOPTON and P. SALTMAN, *Inorg. Chim. Acta*, **242** (1996) 57.
38. R. W. WILSON and M. GROSELL, *Biochim. Biophys. Acta*, **1618** (2003) 163.
39. X. YIN and M. J. STOTT, *J. Chem. Phys.* **118** (2003) 3717.
40. K. ONUMA and A. ITO, *Chem. Mater.* **10** (1998) 3346.
41. Y. F. CHOU, W. A. CHIOU, Y. XU, J. C. Y. DUNN and B. M. WU, *Biomaterials* **25** (2004) 5323.
42. X. LU and Y. LENG, *Biomaterials* **25** (2004) 1779.
43. G. TREBOUX, P. LAYROLLE, N. KANZAKI, K. ONUMA and A. ITO, *J. Phys. Chem. A* **104** (2000) 5111.
44. B. D. BOYAN, Z. SCHWARTZ, C. H. LOHMANN, V. L. SYLVIA, D. L. COCHRAN, D. D. D. DEAN and J. E. PUZAS, *J. Orthop. Res.* **4** (2003) 638.
45. S. M. REA, R. A. BROOKS, A. SCHNEIDER, S. M. BEST and W. BONFIELD, *J. Biomed. Mater. Res.* **70B** (2004) 250.
46. M. J. DALBY, L. DI SILVIO, G. W. DAVIES and W. BONFIELD, *J. Mater. Sci. Mater. M.* **12** (2000) 805.
47. J. S. SUN, Y. H. TSUANG, C. J. LIAO, H. C. LIU, Y. S. HANG and F. H. LIN, *J. Biomed. Mater. Res.* **37** (1997) 324.
48. C. G. SIMON, W. F. GUTHRIE and F. W. WANG, *ibid.* **68A** (2004) 628.
49. D. P. PIOLETTI, H. TAKEI, T. LIN, P. V. LANDUYT, Q. J. MA, S. Y. KWON and K. L. P. SUNG, *Biomaterials* **21** (2000) 1103.